

## APPLICATION OF BAYESIAN FE MODEL SELECTION FOR SHM OF A MONUMENTAL MASONRY PALACE THROUGH SEMI-SUPERVISED LEARNING

L. Ierimonti<sup>1</sup>, N. Cavalagli<sup>2</sup>, E. García-Macías<sup>2</sup>, I. Venanzi<sup>2</sup>, F. Ubertini<sup>2</sup>

<sup>1 2</sup> Department of Civil and Environmental Engineering, University of Perugia.  
address: Via G. Duranti, 93 - 06125 Perugia, Italy  
e-mail: {laura.ierimonti,nicola.cavalagli,enrique.garciamacias,ilaria.venanzi,filippo.ubertini}@unipg.it

---

**Abstract.** *The identification of high-fidelity surrogate models for real-time updating based on continuous monitoring data, is an emerging and challenging topic in the structural system identification of historical structures with a special focus on damage identification and structural health monitoring. Indeed, the protection of the historical and cultural heritage aimed at developing cost-effective and long-lasting dynamic monitoring systems in regions characterized by high seismic risk, has received a growing attention in civil engineering. A dynamic monitoring system is usually composed by a selected number of sensors installed in strategic positions within the building which enable a continuous assessment of the structural conditions over time. Then, the observation of the recorded data allows to identify any variations due to possible damages, i.e. novelty detection, which is classified as unsupervised learning. The basic idea behind the present paper is to transfer knowledge from data to updated numerical models with varying levels of complexity developed from the engineering judgment in order to detect and localize damage in a probabilistic manner, moving on to semi-supervised learning. In order to accomplish this challenging task, a transfer Bayesian-based learning (TBL) methodology is proposed by means of model class selection. For the purpose, different classes of FE (finite elements) models, with a low level of complexity, are preliminary defined in such a way to reproduce the structural dynamic behavior as a function of damage-dependent mechanical characteristics (such as average elastic moduli) of pre-selected regions within the structure. Such regions, designated as damage-sensitive, are defined on the basis of nonlinear static analyses and/or Engineering judgment. Then, the large amount of measured data is periodically used for the automatic Bayesian model selection procedure, i.e., the inverse problem to derive the posterior statistics of the uncertain parameters over the space of the FE models classes. For verifying the proposed methodology, an iconic monumental palace, located in Gubbio, Italy, named Consoli Palace which has been monitored by the Authors since 2017, is used. The dynamic monitoring system, updated in July 2020, comprises 12 uniaxial accelerometers installed at different levels within the building.*

**Keywords:** Transfer learning, Bayesian model updating, Model Class Selection, Surrogate model, Damage classification, Continuous monitoring.

---

## 1 INTRODUCTION

The non-destructive nature and the relatively low economic impact of the technology make SHM particularly suitable for the detection of structural damages suffered by monumental structures. Nowadays, the most common procedure in civil SHM concerns the data acquisition and feature extraction (system eigenfrequencies and modal shapes) through signal processing [20], while damage identification problems can be classified as a five-level hierarchical approaches [9]: (i) detection; (ii) localization; (iii) classification ; (iv) assessment; (v) prediction. On the one hand, variations over time (novelty detection) in the dynamic response of an healthy structure can be associated to material's damage and deterioration [26], with a special attention to proper techniques able to remove the environmental effects such as temperature and humidity [14] and the different sources of uncertainties related to SHM can be accounted for by means of Bayesian statistical frameworks [28, 1, 27]. On the other hand, long-term monitored data and labeled features able to define the meaning of novelties detection to localize, classify, assess and eventually predict damage are usually not available. Indeed, only a few recent contributions deal with long-term SHM data and damage detection so far [4, 3, 23, 2, 12].

In this context, SHM-based technologies are encompassing machine learning (ML) techniques [18, 17, 24], devoting the attention to the semi-supervised learning paradigm, which allows the use of large amount of monitoring data with and without descriptive labels [5, 6]. The process of prioritizing the acquired data can be accomplished by using numerical models, i.e. precalibrated surrogate models [11, 10], in order to transfer knowledge from the trained model to the data and build a labeled training set. Such methods can be classified as transfer learning (TL) techniques [21, 9, 19].

The present work presents a TBL methodology based on long-term monitoring data aimed at evaluating the possible damage of monumental structures in a probabilistic way. In this framework, TL concepts allow to compensate the lack of labeled structural data, especially in the case of damage occurrence, by means of a trained surrogate model, which is used as a formal prior belief for damage assessment. Then, a Bayesian-based procedure allows to associate a probability of damage occurrence.

The effectiveness of the proposed methodology is demonstrated by making use of a real complex historical masonry building as a case study, the Consoli Palace located in Gubbio, near Perugia, in Italy. The structure has been monitored by the Authors since 2015. The continuous monitoring data are used for the Bayesian-based updating of specific mechanical properties of some pre-selected damage-sensitive regions by means of non-linear static analysis (NLSA) and Engineering judgment (EJ). A trained surrogate model allows to reconstruct different classes of FE models, with a low level of complexity, i.e., depending on a single uncertain parameter. The results show the advantage of having long-term monitoring data on the correct estimation of the uncertain parameters' distribution enabling informed model-based decisions and providing a basis to mitigate the risk of a false alarm. The rest of the paper is organized as follows. Section 2 presents the proposed methodology. Section 3 presents the case study. Section 4 summarizes numerical results. Section 5 concludes the paper.

## 2 THE PROPOSED METHODOLOGY

The proposed methodology, designated as TBL, schematically represented in Figure 1, embraces different consequential steps which can be summarized as follows:

1. Start continuous SHM.

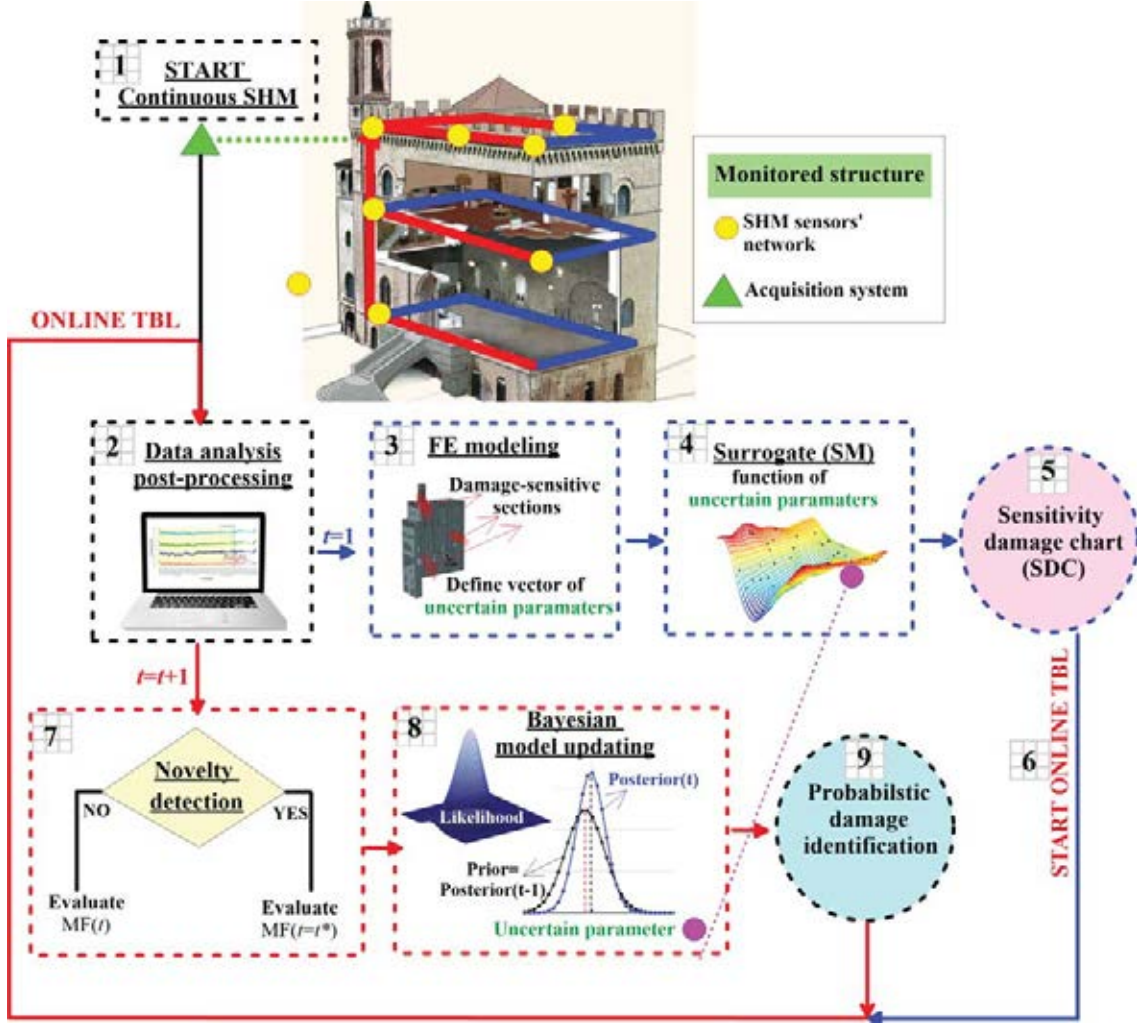


Figure 1: The proposed TBL methodology.

2. Data analysis and post-processing consisting of acquiring data from the monitoring system (acceleration data, temperature information, crack amplitudes) and post-processing data continuously over time to estimate the modal features (MF), such as natural frequencies  $f_i^{\text{exp}}$ , mode shapes  $\Phi_i^{\text{exp}}$  and damping coefficients  $\zeta_i^{\text{exp}}$  associated with each natural vibration mode.
3. If  $t=1$ , where the term  $t$  stands for discrete time (days): FE modeling and evaluation of damage-sensitive regions. The calibration process consists of solving the following optimization problem:

$$\mathbf{Y}^{\text{opt}} = \arg \min_{\mathbf{Y}} \sum_{i=1}^M p_1 \eta_{f,i}(\mathbf{Y}) + p_2 \eta_{\Phi,i}(\mathbf{Y}) \quad (1)$$

where  $M$  is the number of vibration modes;  $\mathbf{Y} = \{\mathbf{Y}_1, \dots, \mathbf{Y}_u, \dots, \mathbf{Y}_U\}$  is the vector collecting the  $n^{\text{th}}$  parameter to be calibrated with  $N$  total number of uncertain parameters;  $p_1$  and  $p_2$  are the weights of the objective function;  $\eta_{f,i}(\mathbf{Y}) = |f_i^{\text{exp}} - f_i^{\text{FEM}}|/f_i^{\text{exp}}$  and  $\eta_{\Phi,i}(\mathbf{Y}) = 1 - \text{MAC}_i(\mathbf{Y})$  are the frequency-based and mode shape-based residual func-

tions, where the term  $MAC_i$  refers to the Modal Assurance Criterion (MAC) between the  $i^{\text{th}}$  experimental  $\Phi_i^{\text{exp}}$  and numerical  $\Phi_i^{\text{FEM}}$  mode shape.

With the main objective of selecting  $j^{\text{th}}$  damage-prone regions  $\mathcal{R} = \{\mathcal{R}_1, \dots, \mathcal{R}_j, \dots, \mathcal{R}_N\}$  with  $j = 1, \dots, N$ , both EJ and NLSA are used. Then, each region is considered as an homogeneous portion of the structure in terms of material and, consequently, potential damage. Hence vector  $\mathbf{X} = \{k_1, \dots, k_j, \dots, k_N\}$  is defined, collecting the multipliers of the Young moduli ( $k_j$ ) of all the elements comprised in each region, with  $0 \leq k_j \leq 1$ .

4. Calibration of the surrogate model as a function of  $\mathbf{X}$ . For the present paper, the Kriging model is used, whose effectiveness in spatial interpolation was demonstrated in previous works by the Authors [11]. According to the Kriging model, the FE model-based data  $\mathbf{X}$  can be numerically interpolated by considering a regression model  $\mathcal{F}$ , i.e., the deterministic component, and an approximation error  $\alpha$ , i.e., the stochastic component [15]:

$$y(\mathbf{X}) = \mathcal{F}(\beta, \mathbf{X}) + \alpha(\mathbf{X}) \quad (2)$$

where  $\beta$  are the regression parameters of  $\mathcal{F}$ . The approximation error  $\alpha$  is assumed as a random process with zero mean and covariance  $\text{cov}(X_i, X_j) = \sigma^2 \mathcal{R}(\boldsymbol{\theta}, X_i, X_j)$ , with  $\sigma^2$  variance of  $\mathcal{F}(\beta, \mathbf{X})$  and  $\mathcal{R}$  the matrix of stochastic-process correlations with components  $r(\boldsymbol{\theta}, X_i, X_j)$ , where  $\boldsymbol{\theta}$  are the correlation parameters.

5. Construction of the SDC, i.e., a graphical chart able to directly associate a stiffness reduction to each frequency/MAC decay for the selected damage-prone region.
6. if  $t > 1$ : novelty detection on a daily basis  $t$ , i.e. daily average values of MF. If a novelty is detected, i.e., a frequency or MAC anomaly, increase the frequency of the modal tests on a hourly basis  $t = t^*$ , i.e.,  $\text{MF}(t^*)$ .
7. Bayesian model updating of the uncertain parameters by means of the surrogate model. Assuming that the identified model parameters  $k_j$  are statistically independent [13, 4], the surrogate model  $\text{SM}(\mathbf{X})$  can be subdivided in  $j$  surrogate models with a low level of complexity, depending on  $k_j$ , i.e.,  $\text{SM}(k_j)$ . Hence, the  $t$ - and  $k_j$ -dependent posterior probability density function (PDF) can be evaluated as follows:

$$p(k_j | \mathbf{d}, t) = c \cdot p(\mathbf{d} | k_j, t) \cdot p(k_j | \mu(t-1)) \quad (3)$$

where  $c = 1 / \int p(\mathbf{d} | k_j, t) p(k_j | \mu(t-1)) dx$  is a normalizing factor called the evidence of the  $\text{SM}(k_j)$ ;  $p(\mathbf{d} | k_j, t)$  is the likelihood function that quantifies the agreement between the measured data  $\mathbf{d}$  and the surrogate-based data;  $p(k_j | \mu(t-1))$  is the prior PDF of  $k_j$  function of the mean value of the posterior  $k_j$  evaluated at  $t-1$ .

More in depth, the likelihood function  $p(\mathbf{d} | k_j, t)$  is modeled as a Gaussian distribution with zero mean [13, 4] as follows:

$$p(\mathbf{d} | k_j, t) = \frac{1}{\left[ 2\pi \prod_{i=1}^M (\sigma_{f_i} \sigma_{\Phi_i})^2 \right]^{(MD)/2}} \exp \left( -\frac{1}{2} \sum_{m=1}^D \sum_{i=1}^M J_i^{\text{err}}(k_j, d_k, t) \right) \quad (4)$$

where index  $i = 1, \dots, M$  refers to the reference parameter associated to the  $i^{\text{th}}$  vibration mode; index  $k = 1, \dots, D$  represents the number of measured data collected in the vector  $\mathbf{d}$ ;  $J_i^{\text{err}} = (\sigma_{f_i})^{-2} e_{f_i}^2(\mathbf{X}, \mathbf{d}) + (\sigma_{\Phi_i})^{-2} e_{\Phi_i}(\mathbf{X}, \mathbf{d})$  is the measure of the fit function (error function) which quantifies the discrepancy between the experimental data and the FE model results with  $\sigma_{f_i}$ ,  $\sigma_{\Phi_i}$  standard deviations associated to the  $i^{\text{th}}$  natural frequency and vibration mode,  $e_{f_i} = f_i^{\text{exp}} - \hat{f}_i(\mathbf{X})$  and  $e_{\Phi_i} = 1 - MAC_i$ .

Finally, it is noteworthy that, theoretically, the prior distribution acts as a regulator in the Bayesian-based model updating process and the more the number of data increases, the less new data influences the updating process. This aspect can be counter-productive, especially in the case of possible damage occurrence. Hence, the co-variance of the prior distribution is assumed as known, while the mean value  $\mu$  is updated step by step, given the evidence of the knowledge acquired at the previous step.

8. Probabilistic damage identification which consists of calculating the probability  $P_j^{\text{dam}}$  that the updated  $j$ th parameter  $k_j^{\text{up}}$  in a possibly damaged state is reduced from the undamaged state  $k_j^{\text{ref}}$  [4, 25]:

$$P_j^{\text{dam}} = P(k_j^{\text{up}} \leq (1 - \bar{k}_j)k_j^{\text{ref}} | \mathbf{d}^{\text{ref}}, \mathbf{d}^{\text{dam}}) = F\left(\frac{(1 - \bar{k}_j)k_j^{\text{ref}} - k_j^{\text{up}}}{\sqrt{(1 - \bar{k}_j)^2 \sigma_{k_j^{\text{ref}}}^2 + \sigma_{k_j^{\text{up}}}^2}}\right) \quad (5)$$

where  $F(\cdot)$  is the standard Gaussian cumulative distribution function;  $\bar{k}_j \in [0, 1]$  is the damage threshold selected for the  $j$ th damage-prone region and quantifies the reduction of  $k_j^{\text{ref}}$ ;  $k_j^{\text{ref}} = 1$  is the reference undamaged state. The possible outcomes of Eq. (5) are summarized in Table 1, where  $P_j^{\text{al}}$  is defined as probability alarm threshold.

No.	Outcome	$P_j^{\text{dam}}$	Meaning
1	$k_j^{\text{up}} = (1 - \bar{k}_j)k_j^{\text{ref}}$	$P_j^{\text{dam}} = 0.5 = P_j^{\text{al}}$	the damage threshold is reached
2	$k_j^{\text{up}} > (1 - \bar{k}_j)k_j^{\text{ref}}$	$P_j^{\text{dam}} < 0.5$	the damage threshold is not reached
3	$k_j^{\text{up}} < (1 - \bar{k}_j)k_j^{\text{ref}}$	$P_j^{\text{dam}} > 0.5$	the damage threshold is exceeded

Table 1: Possible outcomes of Eq. (5).

Additionally, in order to capture a possible damage occurrence, the damage factor DF is introduced and defined as follows:

$$DF = \frac{k_j^{\text{ref}} - k_j^{\text{up}}}{\bar{k}_j} \quad (6)$$

From Eq. (6) it is possible to obtain  $DF=0$  if  $k_j^{\text{up}} = k_j^{\text{ref}}$  and  $DF=1$  if  $k_j^{\text{ref}} - k_j^{\text{up}} = \bar{k}_j$ . If  $DF>1$ , it means that  $k_j^{\text{up}}$  is strongly reduced with respect to the threshold  $\bar{k}_j$ , which is a sign of a possible high level of damage for region  $j$  or a possible false alarm due the lack of consistency with a damage in the  $j$ th region. Hence, the case of  $DF>1$  needs to be carefully checked in real world in order to avoid false alarms.



### 3 THE CASE STUDY: THE CONSOLI PALACE

The Consoli Palace is a medieval building with a rectangular plan and a height of 60 meters above the square level, located in Gubbio, Umbria, central Italy. With reference to Figure 2, three structural components can be identified: a central body; a loggia, connected to the main structure along the south wall; a bell tower. The architectural style of each façade (East and West side), is characterized by round arched windows and merlons in the rooftop. The load-bearing walls have a thickness of about 1.2 m and they are connected through horizontal masonry vaults. The Palace is built in calcareous stone masonry with a regular and homogeneous texture.

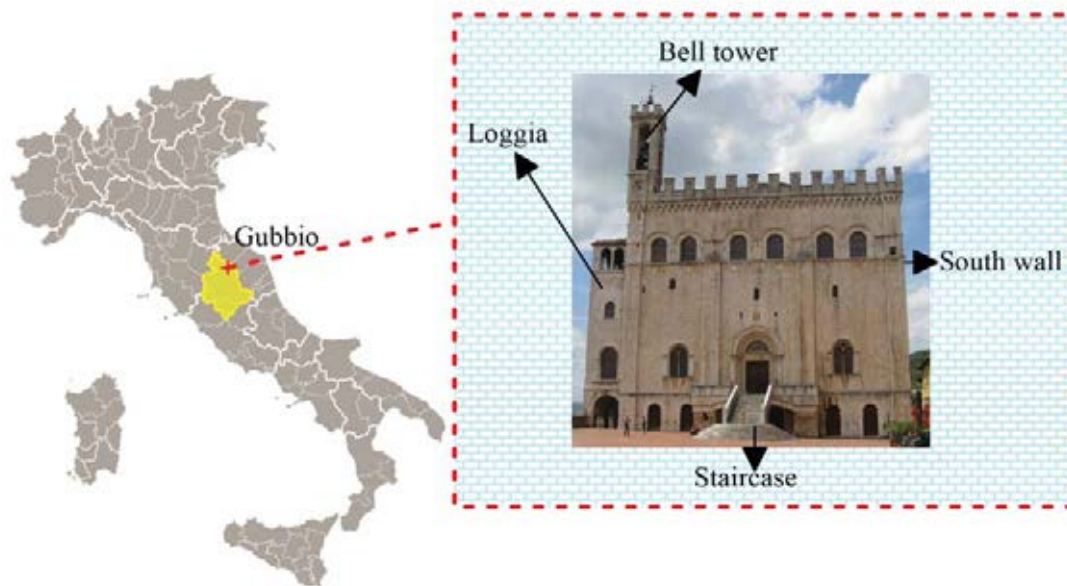


Figure 2: The Consoli Palace, located in Gubbio, Umbria, central Italy.

#### 3.1 The SHM system

The monitoring system (Figure 3) was installed and activated by the Department of Civil and Environmental Engineering of University of Perugia in July 2020. Data are stored every 30 minutes with an acquisition sampling frequency of 40 Hz. The SHM system is characterized by:

1. No. 1 NI CompactDAQ-9132 data acquisition system to which sensors A1-A12, C1-C2 and T1-T2 are wired;
2. No. 1 wireless gateway to which sensors C3,C4,T3-T6 are connected;
3. No. 12 PCB393B12 unidirectional accelerometers A1-A12, differently oriented, installed at the 3rd (A7, A8 and A9), 5th (A4, A5 and A6), roof level (A1, A2, A3, A11 and A12) and wired to the acquisition system through NI 9234 acquisition module;
4. No. 4 S-series linear variable transducers (LVDTs), denoted as C1-C4. Sensors C1-C2 are wired to the acquisition system by means of a NI 9219 acquisition modules;
5. No. 6 temperature sensors T1-T6.

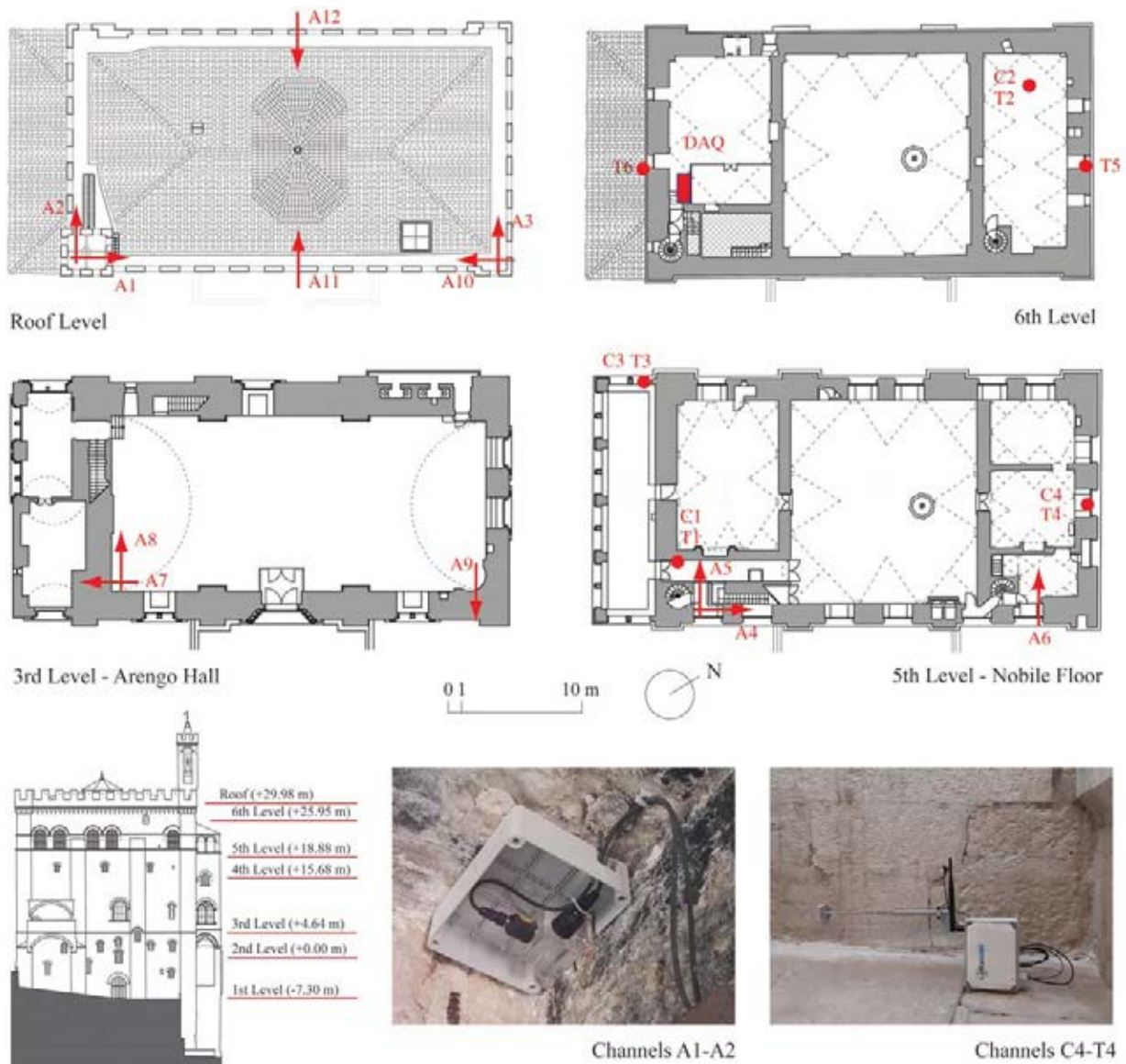


Figure 3: Continuous monitoring configuration.

For the numerical simulations, data stored between July 20<sup>th</sup> 2020 and December 21<sup>th</sup> 2020 are used. The training period is set between July 20<sup>th</sup> 2020 and November 15<sup>th</sup> 2020). Environmental effects are removed by using Multiple Linear Regression (MLR) by means of the least-angle regression (LAR) algorithm [8], which allows to efficiently select the predictors. It is worth noticing that a training period of 1 year would be more appropriate in order to effectively remove environmental effects.

### 3.2 FE model

According to Sect 2, step 3, a 3D FE model of the structure has been built and calibrated within the Abaqus environment [22] in order to reproduce local and global modes of vibration identified at  $t = 1$ . The masonry of the Palace is modeled by means of tetrahedral elements with isotropic materials. The well known concrete damage plasticity (CDP) model is assigned to reproduce the non-linear behavior and the assumed mechanical parameters are summarized as follows [16]:

- parameter which regulates the shape of the yield surface  $K_c = 0.667$  (Lubliner criterion);
- eccentricity term  $e = 0.1$ ;
- ratio between the ultimate compression strength in biaxial stress states and in uniaxial conditions  $r = 1.16$ ;
- viscosity parameter  $\nu = 0.002$ .

Table 2 illustrates the principal vibration modes of the Consoli Palace: Fx1 is a global flexural mode along the  $x$  direction ; Fy1 is a global flexural mode along the  $y$  direction; L1 is a local mode which pertains to the bell tower; T1 is a global torsional mode. The  $x$  and  $y$  directions develop along the longer side and the shorter side of the Palace, respectively. The relatively low quality of model calibration, i.e., values of MAC lower than 0.8, has been already discussed in [14, 7].





Mode Fx1	Mode Fy1	Mode L1	Mode T1
			
$f_1 = 2.35 \text{ Hz}$ $\text{MAC}_1 = 0.98$	$f_2 = 3.05 \text{ Hz}$ $\text{MAC}_2 = 0.76$	$f_3 = 3.46 \text{ Hz}$ $\text{MAC}_3 = 0.64$	$f_4 = 4.17 \text{ Hz}$ $\text{MAC}_4 = 0.97$

Table 2: FE model-based frequencies and MAC of principal vibration modes.

### 3.3 FE model-based damage prone regions

Damage-prone regions are selected by means of NLSA and EJ. More in detail, each selected region allows to define a one-parameter dependent model. The different models (1-6) are described in Table 3.

Model No.	Region	Description	Uncertain Parameter	Source
1	R1	Loggia	$k_1$	EJ
2	R2	Crack pattern $x$	$k_2$	NLSA
3	R3	Crack pattern $y$	$k_3$	NLSA
4	R4	Bell tower	$k_4$	EJ
5	R5	Staircase	$k_5$	EJ
6	R6	main façade's degradation	$k_6$	EJ

Table 3: The different model selected by means of NLSA and EJ.

In particular: R1 represents the poor connection exerted between the loggia and the central body of the Consoli Palace (Figure 4a); R2 represents the crack pattern resulting from NLSA along  $x$  direction capable of reproducing the existing pattern, especially along the south wall



(Figure 4b); R3 refers to the crack pattern resulting from NLSA along the  $y$  direction (Figure 4c); R4 pertains to the bell tower (Figure 4d); R5 represents a possible damage to the principal staircase (Figure 4e); R6, which represents degradation of the exterior texture of the main façade of the building (Figure 4f) due to climate-induced material aging [7].

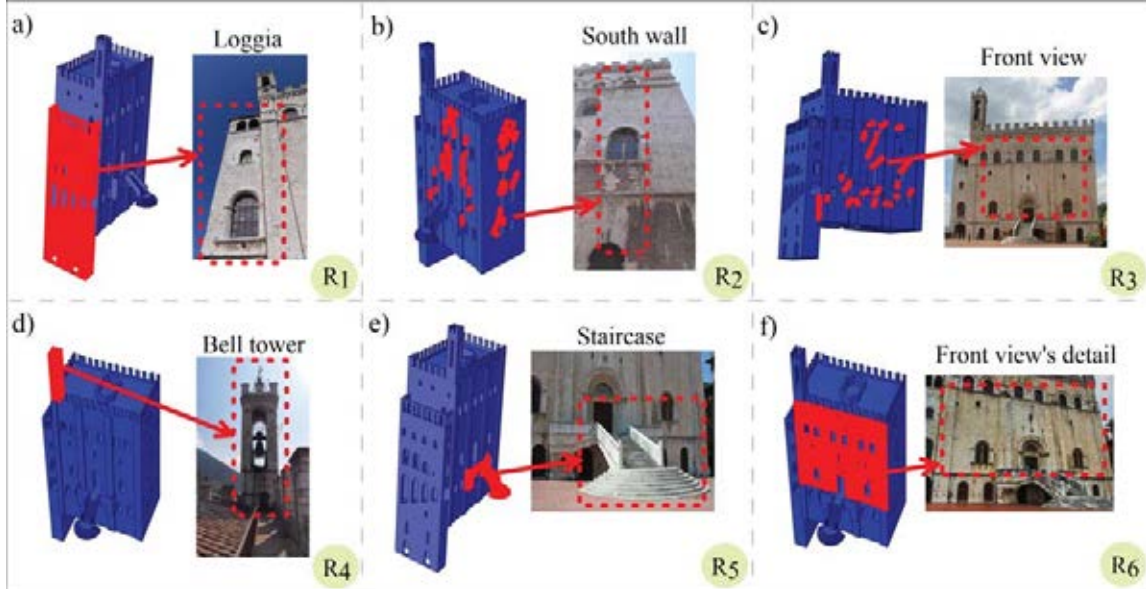


Figure 4: Selected damage sensitive areas with reference to both FE model and real structure: a) R1, the loggia; b) R2, crack pattern  $y$ ; c) R3, crack pattern  $x$ ; d) R4, the bell tower; e) R5, the staircase; f) R6, the façade degradation.

As reported in Table 3, in such areas, the multipliers of the Young's moduli ( $k_1, \dots, k_6$ ) assigned to the isotropic material of each region are assumed as uncertain. In order to calibrate the surrogate model, a total number of 500 samples ( $N_s$ ) are randomly simulated for the uncertain parameters collected in vector  $\mathbf{X}$ . The correspondence between both frequencies and mode shapes is quantified by calculating the coefficient of determination  $R^2$  and the function  $J_{MAC} = 1/N_s \sum_i (1 - MAC_i)$  by comparing the FE and the Kriging models, respectively. Values of  $R^2$  and  $J_{MAC}$  are summarized in Table 4. From the Table it can be noted

Parameter	Vibration modes			
	Fx1	Fy1	L1	T1
$R^2$	0.9833	0.997	0.999	0.9968
$J_{MAC}$	0.0142	0.0015	0.0156	5.85E-5

Table 4: Values of  $R^2$  and ( $J_{MAC}$  associated with the calibrated surrogate model.

that the surrogate-predicted frequencies and mode shapes (Kriging estimate) well fit the corresponding FE values.

#### 4 NUMERICAL RESULTS

The SM-based sensitivity damage chart SDC, which relates frequency and MAC values with the uncertain parameters for each Model, is depicted in Figure 5. On the one hand, due to the observed frequency decay, Fx1 (flexural mode along the  $x$  direction) appears as the most

damage-sensitive vibration mode for damage-prone regions R2 and R5, Fy1 (flexural mode along the  $y$  direction) for R1, R3, R4 and R6, L1 (local mode which pertains to the bell tower) for R4 and R6, and T1 (torsional mode) for R1 and R2. On the other hand, it can be observed that MAC variations can be considered negligible for all damage-prone regions except for R1 and R4. Indeed, a reduction of  $k_1$  provokes a modification in the local L1 mode shapes and a reduction of  $k_4$  induces a huge reduction of Fy1 and L1 MAC values.

Finally, a damage scenarios (Table 5), designated as DII, is selected for the numerical analyses

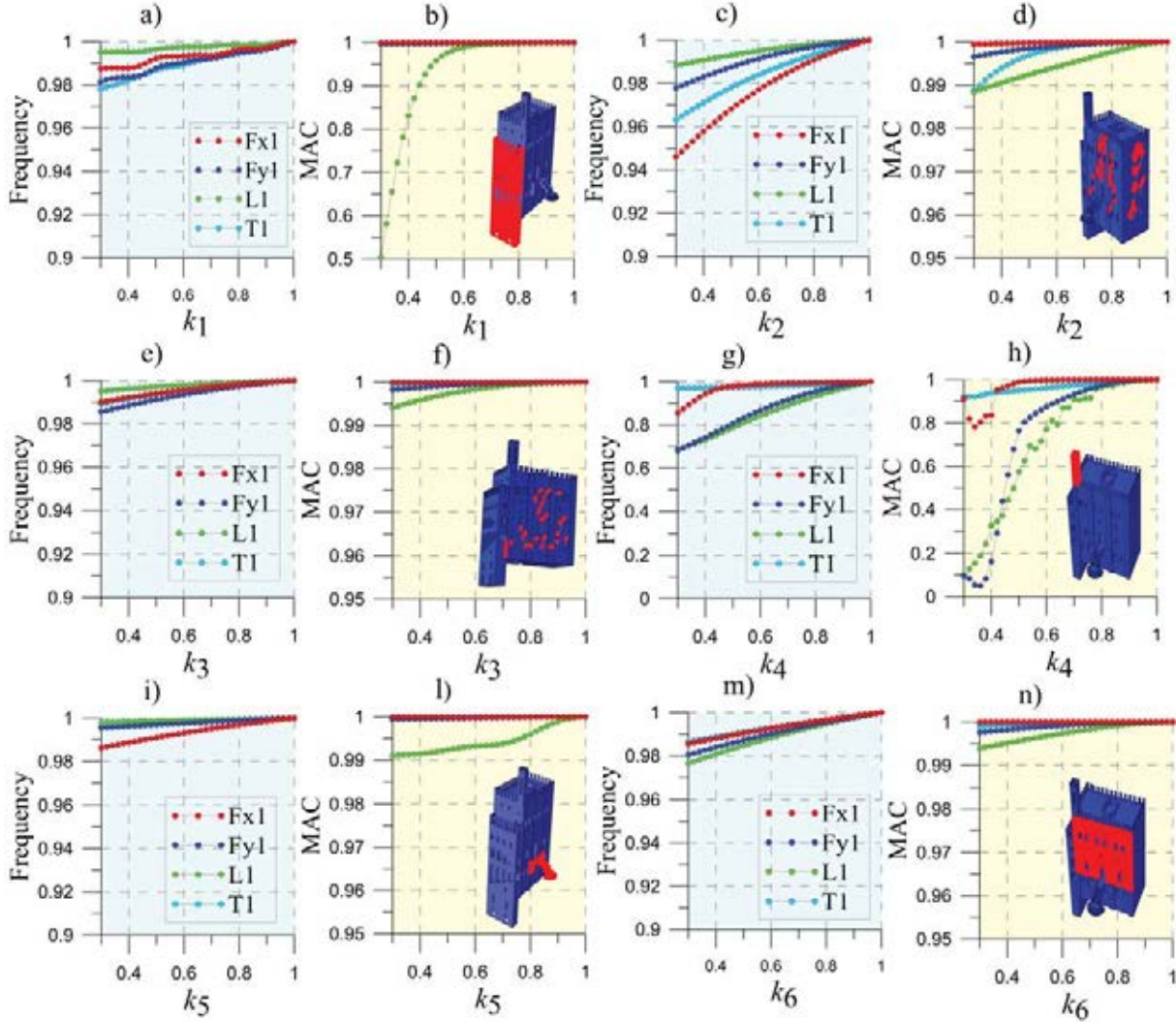


Figure 5: SDC for frequency and MAC decays: a)-b) R1; c)-d) R2; e)-f) R3; g)-h) R4; i)-l) R5; m)-n) R6.

by artificially simulating the frequencies decays (reported in Table 5) extracted from the SDC of region R2 in correspondence with the value of  $k_2 = 0.3$ , while MAC decays are negligible.

Following, the main results of the Bayesian model updating are summarized by simulating damage scenario DII. The uncertain parameter  $k_2$  is updated once the model is trained, i.e., starting from November 15<sup>th</sup> 2020. From that moment on, the monitored data are gathered together in subgroups of daily data-sets ( $t$ ) in order to perform the Bayesian model updating continuously over time on a daily basis. The first 20 days are considered as undamaged. Then, a damage scenario is simulated and the frequency of the model updating is incremented on an hourly basis ( $t^*$ ), as described in Sect. 2.

Damage scenario	Uncertain parameter						Frequency decays			
	$k_1$	$k_2$	$k_3$	$k_4$	$k_5$	$k_6$	Fx1	Fy1	L1	T1
DII	1	0.3	1	1	1	1	0.054	0.022	0.012	0.037

Table 5: Values of  $k_j$  representing the different damage scenarios and corresponding frequency and MAC decays (%).

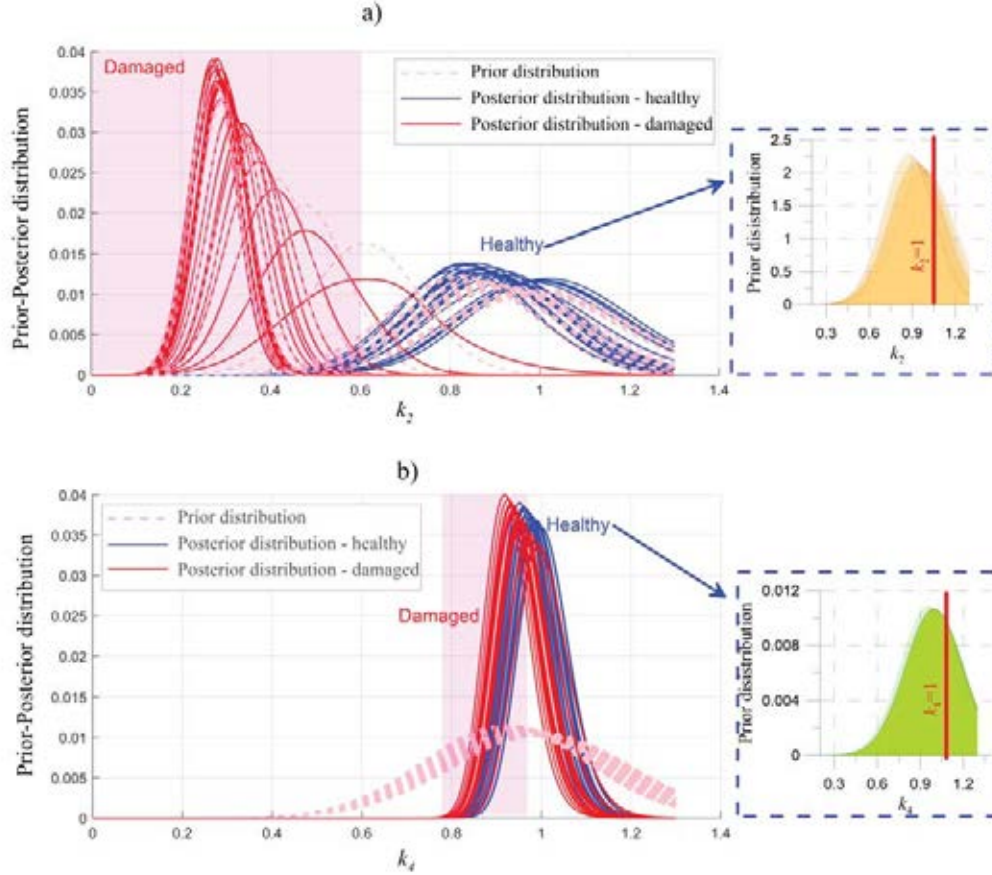


Figure 6: Bayesian-based prior and posterior distributions by simulating damage scenario DII for  $k_2 = 0.3$ : a) R2; b) R4.

Results in terms of prior and posterior distributions for  $k_2$  and  $k_4$ , when DII is simulated, are depicted in Figures 6a)-b). From the results it can be observed that the posterior distributions associated to the uncertain parameters  $k_2$  and  $k_4$  in the undamaged time period present a fluctuation of the mean value of  $k_j$  between about 0.9 and 1. This aspect can be related to the fact that  $k_j$  is sensitive to the slight variations which can daily occur in the frequency and, eventually, MAC tracking as confirm by the SDC. This sensitivity to changing environmental conditions can be considerably reduced by considering an appropriate training period, i.e., 1 year. Moreover, consistently with the SDC, the occurrence of a damage for region R2 is clearly highlighted by a translation of the posterior curves towards reduced values of the selected uncertain parameter  $k_2$  (Figure 6a). In detail, it can be observed that the Bayesian-based procedure is able to tracing back to the simulated damage scenario associated to R2, i.e.,  $k_2^{\text{up}} \approx 0.3$ . However, as expected, the simulation of DII barely affects  $k_4$  (bell tower) in the damaged state (Figure 6b), since the mean value of the posterior distribution doesn't significantly change between healthy and damaged conditions.

As concerns the probabilistic damage identification, Figures 7a)-f) illustrate the updated values



of the uncertain parameters  $k_j^{\text{up}}$  over the number of updates, while Figures 7g)-n) show the trend of DF vs  $P^{\text{dam}}$ , when simulating the occurrence of damage scenario DII. According to the SDC, the simulated frequency decays are reported in Table 5. The values of  $\bar{k}_j$  selected for the eval-

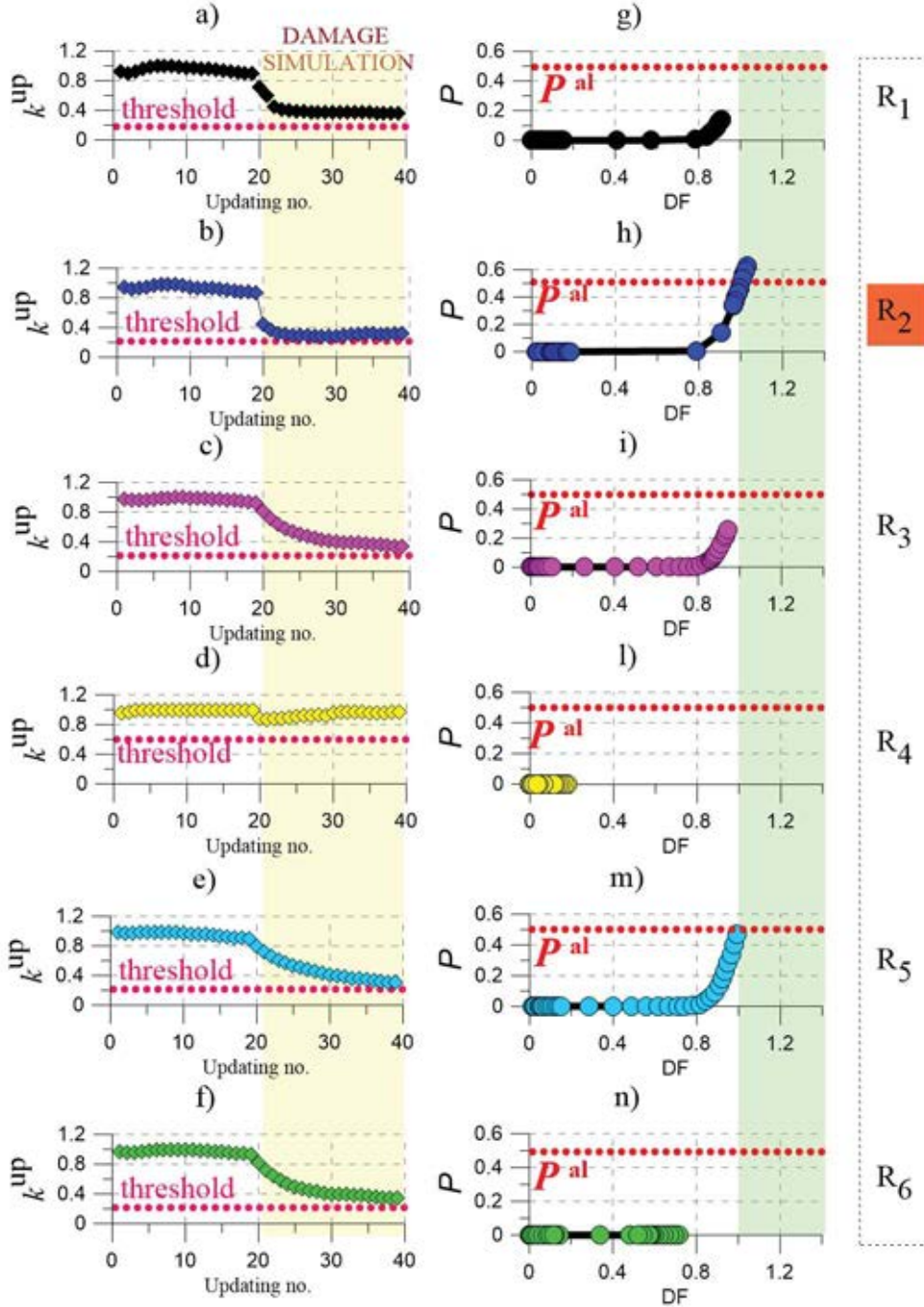


Figure 7: Time series of  $k_j^{\text{up}}$  over the number of updates by simulating the occurrence of the damage scenario DII (Table 5 for each damage-prone region, with the indication of  $P^{\text{al}}$  and  $\bar{k}_j$ : a) R1; b) R2; c) R3; d) R4; e) R5; f) R6.

uation of DF and  $P^{\text{dam}}$  are the following: a) R1:  $\bar{k}_1 = 0.7$ ; b) R2:  $\bar{k}_2 = 0.7$ ; c) R3:  $\bar{k}_3 = 0.7$ ; d) R4:  $\bar{k}_4 = 0.4$ ; e) R5:  $\bar{k}_5 = 0.7$ ; f) R6:  $\bar{k}_6 = 0.7$ . Region R4 pertains to the bell tower and a reduction of the bell tower's stiffness corresponding to 40 % ( $k_4 = 0.6$ ) is assumed sufficient to simulate a damage occurrence. From the Figures it can be noted that  $P^{\text{al}}$  is reached for region



R2, as expected, and for region R5. This result is consistent with the SDC-based results, since both regions R2-R5 can be designated to damage when a frequency decay of mode Fx1 occurs. The case of R5 deserves a particular attention and needs to be checked in the real-world structure with the main objective to avoid a false alarm. Indeed, after a certain number of updates (see the multiple points in the damaged area),  $P^{\text{dam}}$  tends to 1, DF approaches 1 and  $k_5^{\text{up}}$  faces up to  $1 - \bar{k}_5$ . This fact is due to the higher sensitivity of  $k_5$  to small variations associated to Fx1. On the contrary, the remaining regions exhibit a smaller probability of being damaged, which is consistent with the simulated scenario.

## 5 CONCLUSIONS

The present paper has presented the numerical results of a transfer learning Bayesian methodology in the context of integrated SHM aimed at the probabilistic damage assessment of monumental structures.

The case study building is the Consoli Palace, located in Gubbio, Umbria (Italy), which has been monitored by the Authors since 2015 with an enhancement of the SHM sensors' network in 2020. The dynamic behavior of the Palace is reproduced on a calibrated FE model and NLSA in conjunction with EJ enabled to pick damage-sensitive regions within the structure. Then, each selected region allows to define a one-parameter dependent model, i.e., the multiplier of the Young's Modulus assigned to the isotropic material associated with each region. The surrogate modeling has been performed by using the Kriging model in order to define the region-dependent SDC as a prior knowledge of possible damage. Finally, a real time Bayesian model updating of the selected uncertain parameters has been developed in order to continuously identify the probability of damage occurrence over the selected regions. The main advantages and innovations of the proposed approach concern:

- the use of real-time long-term monitoring data within the context of Bayesian TL where the surrogate modeling allows real-time data;
- the use of damage factors and damage probabilities enabling informed model-based decisions and providing a basis to mitigate the risk of a false alarm.
- the use of NLSA to generate estimates of potentially vulnerable structural regions alongside with EJ.
- the possibility to continuously identify the probability of damage occurrence over time in a timely manner.

## Acknowledgments

The Authors would like to acknowledge the support of the PRIN 2017 project, "DETECT-AGING" (Prot. 201747y73L), funded by the Italian ministry of university and research.

## REFERENCES

- [1] S-K. Au. Uncertainty law in ambient modal identification-part ii: Implication and field verification. *Mechanical Systems and Signal Processing*, 48(1-2):34–48, 2014.

- [2] G. Bartoli, M. Betti, A.M. Marra, and S. Monchetti. A bayesian model updating framework for robust seismic fragility analysis of non-isolated historic masonry towers. *Philosophical Transactions of the Royal Society A: Mathematical, Physical and Engineering Sciences*, 377(2155), 2019.
- [3] I. Behmanesh and B. Moaveni. Accounting for environmental variability, modeling errors, and parameter estimation uncertainties in structural identification. *Journal of Sound and Vibration*, 374:92–110, 2016.
- [4] I. Behmanesh, B. Moaveni, G. Lombaert, and C. Papadimitriou. Hierarchical bayesian model updating for structural identification. *Mechanical Systems and Signal Processing*, 64–65:360–376, 2015.
- [5] L.A. Bull, T.J. Rogers, C. Wickramarachchi, E.J. Cross, K. Worden, and N. Dervilis. Probabilistic active learning: An online framework for structural health monitoring. *Mechanical Systems and Signal Processing*, 134:106294, 2019.
- [6] L.A. Bull, K. Worden, and N. Dervilis. Towards semi-supervised and probabilistic classification in structural health monitoring. *Mechanical Systems and Signal Processing*, 140:106653, 2020.
- [7] N. Cavalagli, A. Kita, V.L. Castaldo, A.L. Pisello, and F. Ubertini. Hierarchical environmental risk mapping of material degradation in historic masonry buildings: An integrated approach considering climate change and structural damage. *Construction and Building Materials*, 215:998–1014, 2019.
- [8] Bradley Efron, Trevor Hastie, Iain Johnstone, and Robert Tibshirani. Least angle regression. *Annals of statistics*, 32(2):407–499, 2004.
- [9] C.R. Farrar and K. Worden. *Structural Health Monitoring: A Machine Learning Perspective*. 2012. John Wiley & Sons, Ltd.
- [10] E. García-Macías, L. Ierimonti, I. Venanzi, and F. Ubertini. Comparison of surrogate models for handling uncertainties in shm of historic buildings. *Lecture Notes in Mechanical Engineering*, pages 1645–1657, 2020.
- [11] E. García-Macías, L. Ierimonti, I. Venanzi, and F. Ubertini. An innovative methodology for online surrogate-based model updating of historic buildings using monitoring data. *International Journal of Architectural Heritage*, 15(1):92–112, 2021.
- [12] L. Ierimonti, I. Venanzi, N. Cavalagli, F. Comodini, and F. Ubertini. An innovative continuous bayesian model updating method for base-isolated RC buildings using vibration monitoring data. *Mechanical Systems and Signal Processing*, 139:106600, 2020.
- [13] J. Jang and A. Smyth. Bayesian model updating of a full-scale finite element model with sensitivity-based clustering. *Structural Control and Health Monitoring*, 24(11):e2004, 2017.
- [14] A. Kita, N. Cavalagli, and F. Ubertini. Temperature effects on static and dynamic behavior of consoli palace in gubbio, italy. *Mechanical Systems and Signal Processing*, 120:180–202, 2019.

- [15] S.N. Lophaven, H.B. Nielsen, and J. Søndergaard. A matlab kriging toolbox, version 2.0. Technical Report IMM-TR-2002-12, Kongens Lyngby, Copenhagen, Denmark: Informatics and Mathematical Modelling, Technical University of Denmark, DTU., 2002.
- [16] G. Milani, M. Valente, and C. Alessandri. The narthex of the church of the nativity in bethlehem: A non-linear finite element approach to predict the structural damage. *Computers and Structures*, 207:3–18, 2018.
- [17] A.C. Neves, I. González, J. Leander, and R. Karoumi. A new approach to damage detection in bridges using machine learning. *Lecture Notes in Civil Engineering*, 5:73–84, 2018.
- [18] A.C. Neves, I. Gonzalez, J. Leander, and R. Karoumi. Structural health monitoring of bridges: a model-free ann-based approach to damage detection. *Journal of Civil Structural Health Monitoring*, 7(5):689–702, 2017.
- [19] T.J. Rogers, K. Worden, R. Fuentes, N. Dervilis, U.T. Tygesen, and E.J. Cross. A bayesian non-parametric clustering approach for semi-supervised structural health monitoring. *Mechanical Systems and Signal Processing*, 119:100–119, 2019.
- [20] L. Rosafalco, A. Manzoni, S. Mariani, and A. Corigliano. Fully convolutional networks for structural health monitoring through multivariate time series classification. *Advanced Modeling and Simulation in Engineering Sciences*, 7(1):38, 2020.
- [21] F. Schwenker and E. Trentin. Pattern classification and clustering: A review of partially supervised learning approaches. *Pattern Recognition Letters*, 37(1):4–14, 2014.
- [22] Simulia. *Abaqus Analysis User’s Manual. Volume III: Materials*. Dessault Systèmes, USA, 2010.
- [23] H. Sun, A. Mordret, G.A. Prieto, M.N. Toksz, and O. Bykztrk. Bayesian characterization of buildings using seismic interferometry on ambient vibrations. *Mechanical Systems and Signal Processing*, 85:468–486, 2017.
- [24] L. Sun, Z. Shang, Y. Xia, S. Bhowmick, and S. Nagarajaiah. Review of bridge structural health monitoring aided by big data and artificial intelligence: From condition assessment to damage detection. *Journal of Structural Engineering (United States)*, 146(5):04020073, 2020.
- [25] M.-W. Vanik, J.-L. Beck, and S.-K. Au. Bayesian probabilistic approach to structural health monitoring. *Journal of Engineering Mechanics*, 126(7):738–745, 2000.
- [26] I. Venzani, A. Kita, N. Cavalagli, L. Ierimonti, and F. Ubertini. Earthquake-induced damage localization in an historic masonry tower through long-term dynamic monitoring and fe model calibration. *Bulletin of Earthquake Engineering*, 18(5):2247–2274, 2020.
- [27] W.-J. Yan and L.S. Katafygiotis. An analytical investigation into the propagation properties of uncertainty in a two-stage fast bayesian spectral density approach for ambient modal analysis. *Mechanical Systems and Signal Processing*, 118:503–533, 2019.
- [28] K.-V. Yuen and L.S. Katafygiotis. Bayesian time-domain approach for modal updating using ambient data. *Probabilistic Engineering Mechanics*, 16(3):219–231, 2001.